Published in final edited form as:
J Magn Reson Imaging. 2009 July ; 30(1): 35–40. doi:10.1002/jmri.21826.

Contrast Enhanced MR Imaging of Carotid Atherosclerosis: Dependence on Contrast Agent

William S. Kerwin, PhD[1], **Xihai Zhao, MD**[1], **Chun Yuan, PhD**[1], **Thomas S. Hatsukami, MD**[2], **Kenneth R. Maravilla, MD**[1], **Hunter R. Underhill, MD**[1], and **Xueqiao Zhao, MD**[3]

[1]Department of Radiology, University of Washington, Seattle, WA 98109

[2]Department of Surgery, University of Washington, Seattle, WA 98109

[3]Division of Cardiology, University of Washington, Seattle, WA 98109

Abstract

Purpose—To investigate the dependence of contrast-enhanced MRI of carotid artery atherosclerotic plaque on use of gadobenate dimeglumine versus gadodiamide.

Materials and Methods—15 subjects with carotid atherosclerotic plaque were imaged with 0.1 mmol/kg of each agent. For arteries with interpretable images, the areas of the lumen, wall, and necrotic core and overlying fibrous cap (when present) were measured, as were the percent enhancement and contrast-to-noise ratio (CNR). A kinetic model was applied to dynamic imaging results to determine the fractional plasma volume v_p and contrast agent transfer constant K^{trans}.

Results—For 12 subjects with interpretable images, the agent used did not significantly impact any area measurements or the presence or absence of necrotic core ($p>0.1$ for all). However, the percent enhancement was greater for the fibrous cap (72% vs. 54%; $p<0.05$) necrotic core (51% vs. 42%; $p=0.12$), and lumen (42% vs. 63%; $p<0.05$) when using gadobenate dimeglumine, although no apparent difference in CNR was found. Additionally, K^{trans} was lower when using gadobenate dimeglumine (0.0846 min^{-1} vs. 0.101 min^{-1}; $p<0.01$), although v_p showed no difference (9.5% vs. 10.1%; $p=0.39$).

Conclusion—Plaque morphology measurements are similar with either contrast agent, but quantitative enhancement characteristics, such as percent enhancement and K^{trans}, differ.

Keywords

contrast-enhanced MRI; atherosclerosis; gadobenate dimeglumine; gadodiamide; dynamic MRI

INTRODUCTION

In the carotid artery and other large vessels, MRI has been shown to provide quantitative information regarding atherosclerotic plaque composition and structure (1). These MRI techniques have been used in numerous investigations, such as clinical studies of therapeutic response in atherosclerotic arteries (2,3), comparative studies of demographic differences in atherosclerotic disease features (4), and prospective studies of plaque features associated with patient outcomes (5). These studies and other histological investigations (6–8) have established key imaging targets for identifying the atherosclerotic plaques that are most likely to lead to patient complications. Among the key targets are the condition of the

Correspondence to: William Kerwin, 815 Mercer Street, Seattle WA, 98109 ,206-616-9347, 206-616-9354 (fax), bkerwin@u.washington.edu.

fibrous cap, the size of the necrotic core, and the extent of inflammatory activity within the plaque.

For quantifying these features, use of an injected gadolinium-based contrast agent can be especially helpful. Contrast agents have been shown to preferentially enhance fibrous areas more than necrotic regions (9). This feature has been used to aid in the detection and measurement of the fibrous cap overlying the necrotic core (10,11), and shown to improve the reproducibility of measurements of necrotic core size (12). Dynamic contrast-enhanced (DCE) MRI of atherosclerotic plaque in human and animal studies has been shown to produce measurements of vascular volume and permeability that strongly associate with inflammatory markers including neovessels (13,14), macrophages (15), and serum C-reactive protein (16).

The dependence of contrast-enhanced analysis of carotid atherosclerosis on the choice of contrast agent has not been evaluated. Among agents approved for clinical use, gadobenate dimeglumine (MultiHance, Bracco, Milan) has considerable potential to yield altered enhancement characteristics because it binds weakly to albumin. This results in an approximately two-fold higher relaxivity compared to other clinically used agents (17), such as gadodiamide (Omniscan, GE Healthcare, Milwaukee, WI). These features have the potential to improve differentiation of fibrotic and necrotic plaque components through higher contrast-to-noise ratios due to greater enhancement. Also, binding to albumin may slow contrast agent transfer to the plaque, reducing the necessary temporal resolution for DCE-MRI evaluations.

The purpose of this investigation was to compare qualitative and quantitative enhancement characteristics of carotid atherosclerotic plaque using two clinically-approved agents: godobenate dimeglumine and gadodiamide.

MATERIALS AND METHODS

Patient Selection

A total of 15 subjects were recruited from an ongoing MRI study of the effects of lipid therapy on carotid atherosclerosis (18). Subjects in that study were recruited based on confirmed coronary or carotid artery disease, assigned to one of three treatments, and imaged at yearly intervals. Patients with chronic renal function impairment, characterized by creatine greater than 1.5 mg/dl, were excluded to prevent complications from use of the contrast agents. Each examination included contrast-enhanced imaging with gadodiamide. From this study, subjects were recruited at the time of their annual scan for a repeat MRI examination with gadobenate dimeglumine if a visual assessment of the imaging results indicated the presence of a carotid lesion of at least AHA type IV (21). The repeat scan was scheduled within 1 week after the annual scan. The study was approved by the institutional review board and all subjects provided informed consent.

MRI Protocol

Both MRI examinations were conducted on a 1.5T MR scanner (Signa Horizon EchoSpeed 5.8, GE Medical Systems) using a custom phased-array carotid surface coil (19). The examination included an axial T1-weighted fast spin echo sequence with a T1-insensitive, quadruple inversion recovery (QIR) black-blood preparation (20). Relevant imaging parameters for the T1-weighted images were TR=800ms, TE=11ms, TI1=375ms, TI2=126ms, thickness=2mm, gap = 0mm, field-of-view=16cm×12cm, matrix=256×192, and number of averages=2. A total of 12 slices were obtained centered on the bifurcation of the index carotid artery. Additionally, the examination included a DCE-MRI sequence consisting of axial 2D spoiled gradient-recalled echo imaging without cardiac gating.

Relevant imaging parameters were: TR=100 ms, TE=3.1 ms, flip=60°, thickness=3 mm, gap=1 mm, field-of-view=16×12 cm, and matrix=256×144. Data were simultaneously acquired at six locations, centered on the carotid bifurcation, and at 12 time points separated by a repetition interval of 15 sec. Coincident with the second image in the sequence, 0.1mmol/kg of gadodiamide or gadobenate dimeglumine was injected at a rate of 2 ml/sec by power injector. A spatial saturation band was applied to induce a T1-dependent blood signal resulting in dark blood on images prior to contrast agent arrival. After completion of the DCE-MRI acquisition, the T1-weighted fast spin echo protocol was repeated to obtain contrast-enhanced T1-weighted images.

Image Analysis

Prior to quantitative analysis, all images were reviewed to assess image quality. Subjects with images where the lumen and/or outer wall boundaries were not identifiable in either or both examinations were judged to be of insufficient quality and excluded from the analysis. The remaining subjects were independently reviewed, blinded to the agent used.

The images were evaluated using the CASCADE analysis software (22) by a radiologist (--) with 1 year of experience evaluating MR images of the carotid wall. Lumen and wall boundaries were interactively identified on the post-contrast T1-weighted images. Then, regions of necrotic core were manually drawn using the intensity criteria described by Cai et al. (11). Briefly, a region was considered to be necrotic core if it was iso-intense to hyper-intense relative to adjacent sternocleidomastoid muscle on T1-weighted images and appeared not to enhance on the post-contrast T1-weighted image. The region between the necrotic core and the lumen boundary was considered to be the fibrous cap. For each region identified, the total area and average signal were recorded. For the fibrous cap, the total in-plane length along the lumen boundary was measured. Finally, a remote region in the air space was identified and used to measure the noise level of the image, defined as the standard deviation of the air signal.

Next, the DCE-MRI images were analyzed using kinetic modeling to measure the partial volume of plasma v_p and the transfer constant K^{trans} as described by Kerwin et al. (15). Lumen and outer wall boundaries were mapped from each T1-weighted image onto the corresponding DCE-MRI results and manually adjusted to align with the lumen and wall boundary. The average values of v_p and K^{trans} within the artery wall were recorded. Because DCE-MRI measurements are prone to partial volume effects from the lumen, particularly in regions with little disease, the analysis was limited to locations that had a minimum 2 mm wall thickness over at least 20% of the vessel circumference. Also, pixels immediately adjacent to the lumen boundary were excluded from the measurement.

Data Analysis

Data were compared to evaluate qualitative and quantitative differences between the two contrast agents. Locations were matched based on distance from the carotid bifurcation. The agreement between agents regarding the presence or absence of necrotic core at each location was evaluated using Cohen's κ. Differences in the likelihood of detecting necrotic core were evaluated using McNemar's test. All comparisons were made using the SPSS statistical software package (SPSS Inc., Chicago, IL) with $p<0.05$ taken to indicate significance.

Quantitative measurements were compared for each location using a two-sided paired t-test and their agreement was assessed using the intraclass correlation coefficient (ICC). Quantitative size measurements included areas of the lumen, wall, necrotic core, and fibrous cap, and length of the fibrous cap. Intensity-based measurements included the percentage

enhancement of the lumen, fibrous cap, and necrotic core, the contrast-to-noise ratio (CNR) of the fibrous cap versus the lumen and fibrous cap versus necrotic core, and the DCE-MRI parameters v_p and K^{trans}. Percentage enhancement was defined as the percent change in the average intensity of a region from the pre-contrast T1W image to the post-contrast image.

RESULTS

Of the 15 subjects enrolled, 3 were excluded due to poor image quality, leaving 136 cross-sectional locations for analysis. A representative example of the imaging and analysis results is shown in Figure 1. For all 136 locations, area measurements of the lumen and wall were highly consistent despite the difference in contrast agents (Table 1). No significant difference was observed for the area of the lumen (p=0.48) nor the area of the wall (p=0.22). ICC values were 0.93 and 0.92, respectively, indicating strong agreement.

Detection results for the presence of necrotic cores within each matched location are presented in Table 2. Very good agreement between data sets was observed, indicated by a κ of 0.66. Some of the disagreement was attributable to minor location misalignments resulting in necrotic cores present in consecutive locations. A slightly higher incidence (36 vs. 29 locations, respectively) of necrotic cores was found using gadobenate dimeglumine versus gadodiamide, although this was not significant by McNemar's test (p=0.14). The higher incidence was attributable to three subjects in which small (<5 mm^2) necrotic core regions were only identified using gadobenate dimeglumine. In retrospective comparison, the regions were also found to have signal features consistent with necrotic core based on the gadodiamide images, but the conspicuity was somewhat lower.

In a total of 24 locations, a necrotic core was identified using both contrast agents. Size measurements of the necrotic core and overlying fibrous cap for these 24 locations are also summarized in Table 1. The area of the necrotic core showed good agreement with an ICC of 0.82 and no significant difference (p=0.87). Fibrous cap area had only marginal agreement with an ICC of 0.49, whereas fibrous cap length showed good agreement with an ICC of 0.77. Neither fibrous cap area nor length showed significant differences between measurements (p = 0.70 and 0.25, respectively).

For the 24 locations in which necrotic cores were identified using both agents, percent enhancement characteristics are illustrated in Figure 2. Generally higher enhancement was observed for gadobenate dimeglumine than for gadodiamide. For the fibrous cap, the enhancement increased from 54% to 72% (p<0.05) and for the necrotic core, a non-significant increase from 42% to 51% was observed (p=0.12). Comparing enhancement of the fibrous cap to the necrotic core, the greater enhancement of the fibrous cap was highly significant for both agents (p<0.001 for both). A significant increase in lumen enhancement was also observed from 42% to 63% (p<0.05) owing to the higher relaxivity of gadobenate dimeglumine yielding poorer blood suppression.

The differences in enhancement between agents did not impact the contrast-to-noise ratios of either the fibrous cap versus lumen nor the fibrous cap versus necrotic core. The CNRs for fibrous cap versus lumen were 25.0±15.2 for gadodiamide versus 21.3±8.8 for gadobenate dimeglumine (p=0.27) and for fibrous cap versus necrotic core they were 3.9±6.6 for gadodiamide versus 1.3±3.4 (p=0.07) for gadobenate dimeglumine Although this appears to approach significance in favor of gadodiamide, the difference arose from 3 locations in a single subject where superior coil positioning led to a 2-fold higher CNR. Notably, each agent achieved a higher fibrous cap versus necrotic core CNR than the other in exactly half of all locations.

For the DCE-MRI analysis, 21 locations from 9 subjects met the inclusion criteria. A representative example is shown in Figure 3. Analysis results are summarized in the final two rows of Table 1. Overall, good agreement was observed for measurements of v_p with either agent, resulting in an ICC of 0.84 and no significant difference between measurements ($p = 0.39$). More marginal agreement was exhibited by K^{trans} with an ICC of 0.58. Most importantly, measurements of K^{trans} were significantly smaller with gadobenate dimeglumine compared to gadodiamide ($p<0.01$).

DISCUSSION

This investigation explored the sensitivity of contrast enhanced MRI of atherosclerotic plaque to differences in contrast agents. Several investigations have established the potential of contrast enhanced imaging for plaque characterization (9–16). Wasserman et al. also explored the temporal dependence of enhancement and found relatively little difference in contrast-to-noise ratios over a broad range of delays from a few minutes to half an hour (23). This suggests that delayed contrast enhanced imaging of atherosclerotic plaque is insensitive to the delay time. Previous studies had not, however, established the sensitivity of contrast-enhanced plaque imaging to the choice of contrast agent.

One potential impact of the contrast agent is an effect on measurements of plaque burden. Phan et al. investigated pre and post-contrast T1-weighted imaging of carotid atherosclerosis and found that lumen volume measurements decreased after contrast agent injection, whereas wall volume measurements increased (24). This phenomenon was attributed to enhancement of the vessel boundaries, perhaps due to extensive neovasculature. In this investigation, we found that the lumen and wall measurements were highly consistent whether using gadodiamide or gadobenate dimeglumine. This suggests that the apparent increase in wall volume after contrast agent injection is not impacted by the choice of contrast agent.

The primary utility of contrast-enhanced plaque imaging is to yield better differentiation of plaque components, notably necrotic and fibrous tissues. Because necrotic core size has been implicated in MRI studies of plaque features associated with clinical outcomes (5), contrast-enhanced MRI may be superior to standard MRI for detecting vulnerable plaques. Both Yuan et al. (9) and Wasserman et al. (10) noted higher percent enhancement for fibrous tissue compared to necrotic cores. This led to a contrast-to-noise ratio between the fibrous cap and necrotic core that was significantly higher in post-contrast T1-weighted images than in T2-weighted images (10). In our study, we likewise found significantly higher enhancement of the fibrous cap compared to the necrotic core for both agents. We also found that the percent enhancement of the fibrous cap was significantly higher with gadobenate dimeglumine than with gadodiamide. This can be attributed to the higher relaxivity of gadobenate dimeglumine and suggests that some of the agent remains bound to proteins upon entering the fibrous cap because the higher relaxivity occurs when bound (17).

The increased enhancement did not, however, lead to a higher contrast-to-noise ratio between the fibrous cap and necrotic core. This can be attributed in part to the fact that the necrotic core also enhanced more with gadobenate dimeglumine than with gadodiamide. Thus, the higher relaxivity did not appear to have a net benefit for increased contrast between necrotic and fibrous tissues.

The differential enhancement of necrotic and fibrous regions has been shown by Cai et al. (11) to assist in obtaining accurate measurements of necrotic core areas and by Takaya et al. (12) to reduce reader variability in measuring necrotic core size. In our study, we found that necrotic core area measurements were highly consistent, with no appreciable difference

between contrast agents. A possible trend for identifying more necrotic cores with gadobenate dimeglumine was observed, although this finding was not significant (p=0.14). If true, this finding could be attributable to greater conspicuity of the necrotic core due to higher overall enhancement, but without a gold standard for comparison, the overall accuracy with either contrast agent cannot be assessed.

Cai et al. also used the enhancement of the fibrous cap to identify the fibrous cap region and measure its length and area (11). In this study, we found no difference in measurements of fibrous cap area comparing gadobenate dimeglumine and gadodiamide. However, the agreement between measurements was relatively poor, which we attribute to the intrinsic difficulty in measuring cap area rather than a difference between contrast agents. This difficulty arises because the thickness of the fibrous cap is generally less than 1mm and on the order of the fundamental resolution of the imaging protocol. Measurements of fibrous cap length, on the other hand, appeared more robust with good agreement and no difference attributable to the choice of contrast agent. Whether cap length is clinically meaningful requires further investigation.

In addition to the use of contrast-enhanced imaging to differentiate plaque components, dynamic imaging techniques have also been used to examine contrast agent kinetics in plaque (13–16). Most notably, kinetic modeling to determine the partial plasma volume v_p and transfer constant K^{trans} has shown these parameters to be associated with plaque neovasculature and inflammatory processes (15). Both of these features have been shown to be elevated in plaques associated with patient symptoms (7,8). In comparing kinetic modeling results with gadobenate dimeglumine versus gadodiamide, measurements of v_p showed good agreement and no difference in means. This result is expected given that v_p is determined in this model by the amount of enhancement of plasma within the plaque relative to the enhancement of the lumen; changes in relaxivity have the same effect on plasma signal independent of location so their ratio remains constant. On the other hand, measurements of K^{trans} were significantly lower with gadobenate dimeglumine. The weak binding of this agent to albumin and its higher relaxivity when bound may complicate the kinetics of the agent, leading to the reduction in measured K^{trans}. These factors may potentially be advantageous for gadobenate dimeglumine, because the higher relaxivity may increase the contrast-to-noise ratio and the slower kinetics may allow longer image acquisitions with higher spatial resolution or greater coverage. The agreement between K^{trans} measurements was also somewhat low. The extent to which this is attributable to inherent measurement variability versus differences in the agent is unknown.

Another finding that may impact the choice of contrast agent is that we found higher lumen enhancement with gadobenate dimeglumine than with gadodiamide. This resulted in no improvement in contrast-to-noise ratio between the fibrous cap and lumen despite greater enhancement of the cap. This is due to the higher relaxivity of gadobenate dimeglumine leading to poorer blood suppression and is consistent with similar studies involving delayed enhancement cardiac MRI. These studies have indicated that gadobenate dimeglumine at the same dose as lower relaxivity agents actually reduces the contrast-to-noise ratio between infracted myocardium and the left ventricular cavity (25). Other studies have indicated equivalent myocardial delayed enhancement characteristics can be achieved using lower doses of the agent (26).

The purpose of this study was to investigate to what extent the choice of contrast agent affects atherosclerotic plaque characterization in contrast-enhanced carotid MRI, based on established methods in the literature. Improved measurement methodology, particularly for the DCE-MRI techniques could be used, such as improved temporal resolution or measuring changes in T1 rather than signal intensity to estimate contrast agent concentration. Further

studies are required to investigate the validity of each model or to assess the impact of assumptions used in this study. Nevertheless, the methods used in this study have been found to be histologically meaningful and refined methods are likely to encounter similar sensitivities to the differences in contrast agents observed here. One further limitation of this study is that it only compared two contrast agents, gadodiamide and gadobenate dimeglumine. Thus, direct conclusions can only be drawn for these two agents. Nevertheless, among clinically available agents, these two are among the most different because of differences in relaxivity and binding.

In conclusion, we found that the choice of contrast agent, gadodiamide or gadobenate dimeglumine, had little impact on morphological characterization of carotid atherosclerotic plaque. Detection of necrotic core and quantitative measurements of lumen area, wall area, necrotic core area and fibrous cap size showed no significant differences between agents. On the other hand, measurements involving enhancement characteristics themselves, notably percent enhancement and the kinetic parameter K^{trans}, were significantly affected by the choice of agent. This suggests that measurements of plaque morphology imaged with different contrast agents can be directly compared, but quantitative enhancement characteristics cannot. In longitudinal studies of carotid atherosclerosis, use of the same contrast agent throughout the study is recommended.

Acknowledgments

Funding Sources: Bracco, AHA 0560054Z, NIH RO1 HL073401

References

1. Saam T, Ferguson MS, Yarnykh VL, Takaya N, Xu D, Polissar NL, Hatsukami TS, Yuan C. Quantitative evaluation of carotid plaque composition by in vivo MRI. Arterioscler Thromb Vasc Biol. 2005; 25:234–239. [PubMed: 15528475]
2. Corti R, Fuster V, Fayad ZA, Worthley SG, Helft G, Smith D, Weinberger J, Wentzel J, Mizsei G, Mercuri M, Badimon JJ. Lipid lowering by simvastatin induces regression of human atherosclerotic lesions: two years' follow-up by high-resolution noninvasive magnetic resonance imaging. Circulation. 2002; 106:2884–2887. [PubMed: 12460866]
3. Underhill HR, Yuan C, Zhao XQ, Kraiss LW, Parker DL, Saam T, Chu B, Takaya N, Liu F, Polissar NL, Neradilek B, Raichlen JS, Cain VA, Waterton JC, Hamar W, Hatsukami TS. Effect of rosuvastatin therapy on carotid plaque morphology and composition in moderately hypercholesterolemic patients: a high-resolution magnetic resonance imaging trial. Am Heart J. 2008; 155:584.e1–584.e8. [PubMed: 18294500]
4. Saam T, Cai JM, Cai YQ, An NY, Kampschulte A, Xu D, Kerwin WS, Takaya N, Polissar NL, Hatsukami TS, Yuan C. Carotid plaque composition differs between ethno-racial groups: an MRI pilot study comparing mainland Chinese and American Caucasian patients. Arterioscler Thromb Vasc Biol. 2005; 25:611–616. [PubMed: 15653565]
5. Takaya N, Yuan C, Chu B, Saam T, Underhill H, Cai J, Tran N, Polissar NL, Isaac C, Ferguson MS, Garden GA, Cramer SC, Maravilla KR, Hashimoto B, Hatsukami TS. Association between carotid plaque characteristics and subsequent ischemic cerebrovascular events: a prospective assessment with MRI--initial results. Stroke. 2006; 37:818–823. [PubMed: 16469957]
6. Virmani R, Burke AP, Farb A, Kolodgie FD. Pathology of the vulnerable plaque. J Am Coll Cardiol. 2006; 47:C13–C18. [PubMed: 16631505]
7. McCarthy MJ, Loftus IM, Thompson MM, Jones L, London NJ, Bell PR, Naylor AR, Brindle NP. Angiogenesis and the atherosclerotic carotid plaque: an association between symptomatology and plaque morphology. J Vasc Surg. 1999; 30:261–268. [PubMed: 10436445]
8. Dunmore BJ, McCarthy MJ, Naylor AR, Brindle NP. Carotid plaque instability and ischemic symptoms are linked to immaturity of microvessels within plaques. J Vasc Surg. 2007; 45:155–159. [PubMed: 17210401]

9. Yuan C, Kerwin WS, Ferguson MS, Polissar N, Zhang S, Cai J, Hatsukami TS. Contrast-enhanced high resolution MRI for atherosclerotic carotid artery tissue characterization. J Magn Reson Imaging. 2002; 15:62–67. [PubMed: 11793458]
10. Wasserman BA, Smith WI, Trout HH 3rd, Cannon RO 3rd, Balaban RS, Arai AE. Carotid artery atherosclerosis: in vivo morphologic characterization with gadolinium-enhanced double-oblique MR imaging initial results. Radiology. 2002; 223:566–573. [PubMed: 11997569]
11. Cai J, Hatsukami TS, Ferguson MS, Kerwin WS, Saam T, Chu B, Takaya N, Polissar NL, Yuan C. In vivo quantitative measurement of intact fibrous cap and lipid-rich necrotic core size in atherosclerotic carotid plaque: comparison of high-resolution, contrast-enhanced magnetic resonance imaging and histology. Circulation. 2005; 112:3437–3444. [PubMed: 16301346]
12. Takaya N, Cai J, Ferguson MS, Yarnykh VL, Chu B, Saam T, Polissar NL, Sherwood J, Cury RC, Anders RJ, Broschat KO, Hinton D, Furie KL, Hatsukami TS, Yuan C. Intra- and interreader reproducibility of magnetic resonance imaging for quantifying the lipid-rich necrotic core is improved with gadolinium contrast enhancement. J Magn Reson Imaging. 2006; 24:203–210. [PubMed: 16739123]
13. Kerwin W, Hooker A, Spilker M, Vicini P, Ferguson M, Hatsukami T, Yuan C. Quantitative magnetic resonance imaging analysis of neovasculature volume in carotid atherosclerotic plaque. Circulation. 2003; 107:851–856. [PubMed: 12591755]
14. Calcagno C, Cornily JC, Hyafil F, Rudd JH, Briley-Saebo KC, Mani V, Goldschlager G, Machac J, Fuster V, Fayad ZA. Detection of neovessels in atherosclerotic plaques of rabbits using dynamic contrast enhanced MRI and 18F-FDG PET. Arterioscler Thromb Vasc Biol. 2008; 28:1311–1317. [PubMed: 18467641]
15. Kerwin WS, O'Brien KD, Ferguson MS, Polissar N, Hatsukami TS, Yuan C. Inflammation in carotid atherosclerotic plaque: A dynamic contrast-enhanced MRI study. Radiology. 2006; 241:459–468. [PubMed: 16966482]
16. Kerwin WS, Oikawa M, Yuan C, Jarvik G, Hatsukami T. MR Imaging of Adventitial Vasa Vasorum in Carotid Atherosclerosis. Magn Reson Med. 2008; 59:507–514. [PubMed: 18306402]
17. de Haën C, Cabrini M, Akhnana L, Ratti D, Calabi L, Gozzini L. Gadobenate dimeglumine 0.5 M solution for injection (MultiHance) pharmaceutical formulation and physicochemical properties of a new magnetic resonance imaging contrast medium. J Comput Assist Tomogr. 1999; 23:S161–S168. [PubMed: 10608412]
18. Zhao XQ, Phan BA, Chu B, Bray F, Moore AB, Polissar NL, Dodge JT Jr, Lee CD, Hatsukami TS, Yuan C. Testing the hypothesis of atherosclerotic plaque lipid depletion during lipid therapy by magnetic resonance imaging: study design of Carotid Plaque Composition Study. Am Heart J. 2007; 154:239–246. [PubMed: 17643572]
19. Yarnykh VL, Yuan C. T1-insensitive flow suppression using quadruple inversion-recovery. Magn Reson Med. 2002; 48:899–905. [PubMed: 12418006]
20. Hayes CE, Mathis CM, Yuan C. Surface coil phased arrays for high-resolution imaging of the carotid arteries. J Magn Reson Imaging. 1996; 6:109–112. [PubMed: 8851414]
21. Cai JM, Hatsukami TS, Ferguson MS, Small R, Polissar NL, Yuan C. Classification of human carotid atherosclerotic lesions with in vivo multicontrast magnetic resonance imaging. Circulation. 2002; 106:1368–1373. [PubMed: 12221054]
22. Kerwin W, Xu D, Liu F, Saam T, Underhill H, Takaya N, Chu B, Hatsukami T, Yuan C. Magnetic resonance imaging of carotid atherosclerosis: plaque analysis. Top Magn Reson Imaging. 2007; 18:371–378. [PubMed: 18025991]
23. Wasserman BA, Casal SG, Astor BC, Aletras AH, Arai AE. Wash-in kinetics for gadolinium-enhanced magnetic resonance imaging of carotid atheroma. J Magn Reson Imaging. 2005; 21:91–95. [PubMed: 15611945]
24. Phan BA, Chu B, Kerwin WS, Xu D, Yuan C, Hatsukami T, Zhao XQ. Effect of contrast enhancement on the measurement of carotid arterial lumen and wall volume using MRI. J Magn Reson Imaging. 2006; 23:481–485. [PubMed: 16523478]
25. Schlosser T, Hunold P, Herborn CU, Lehmkuhl H, Lind A, Massing S, Barkhausen J. Myocardial infarct: depiction with contrast-enhanced MR imaging--comparison of gadopentetate and gadobenate. Radiology. 2005; 236:1041–1046. [PubMed: 16055693]

26. Balci NC, Inan N, Anik Y, Erturk MS, Ural D, Demirci A. Low-dose gadobenate dimeglumine versus standard-dose gadopentate dimeglumine for delayed contrast-enhanced cardiac magnetic resonance imaging. Acad Radiol. 2006; 13:833–839. [PubMed: 16777557]

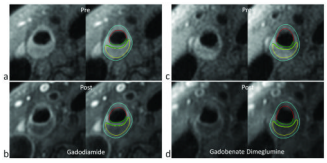

Figure 1.
Similarity of carotid plaque enhancement using gadodiamide (a,b) versus gadobenate dimeglumine (c,d). T1-weighted MR images are shown before (a,c) and after (b,d) injection of 0.1 mmol/kg of the corresponding agent. Each pair shows the images with and without contours corresponding to the lumen (red) outer wall boundary (light blue), necrotic core (yellow) and inner and outer fibrous cap boundaries (green).

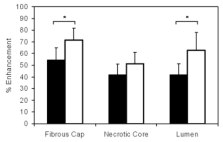

Figure 2.

Percent enhancement characteristics by atherosclerotic plaque tissue type show greater enhancement (*$p<0.05$) for gadobenate dimeglumine (white bars) compared to gadodiamide (black bars). Error bars indicate 95% confidence intervals.

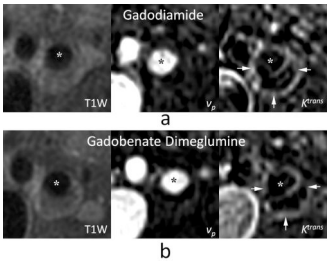

Figure 3.
Kinetic modeling of contrast agent dynamics in carotid atherosclerosis exhibits similar results for gadodiamide (a) versus gadobenate dimeglumine (b). MR images show T1-weighted reference image (left), parametric image of partial plasma volume v_p (middle), and parametric image of the transfer constant K^{trans} (right). Asterisks indicate the carotid artery lumen and arrows indicate a rim of high K^{trans} corresponding to the outer wall boundary.

Table 1

Mean values with significance (P) and intraclass correlation coefficients (ICC) comparing measurements of atherosclerotic plaque made with two contrast agents.

	Mean (standard deviation)				
Measurement*	**Gadodiamide**	**gadobenate dimeglumine**	**P**	**ICC**	**N**
Lumen Area	42.5 (22.6)	43.0 (21.4)	0.48	0.93	136
Wall Area	38.4 (16.4)	37.7 (15.6)	0.22	0.92	136
Necrotic Core Area	8.1 (7.5)	8.2 (7.1)	0.88	0.82	24
Fibrous Cap Area	3.6 (3.3)	3.3 (3.6)	0.70	0.49	24
Fibrous Cap Length	4.6 (2.5)	5.2 (3.0)	0.25	0.77	24
v_p	10.1 (4.5)	9.5 (3.9)	0.39	0.84	21
K^{trans}	0.101 (0.026)	0.0846 (0.017)	0.006	0.58	21

*Area measurements in mm^2, length measurements in mm, v_p in percent, and K^{trans} in min^{-1}.

Table 2

Detection of necrotic cores comparing use of gadodiamide to gadobenate dimeglumine.

	Gadobenate Dimeglumine		
Gadodiamide	**present**	**absent**	**total**
present	24	5	29
absent	12	95	107
total	36	100	136